International Journal of
*Molecular Sciences*

MDPI

*Article*

# Decreased Bone Volume and Bone Mineral Density in the Tibial Trabecular Bone Is Associated with *Per2* Gene by 405 nm Laser Stimulation

**Yeong-Min Yoo [1,†], Myung-Han Lee [2,†], Ji Hyung Park [1], Dong-Hyun Seo [1], Sangyeob Lee [1], Byungjo Jung [1], Han Sung Kim [1] and Kiho Bae [2,*]**

Received: 2 September 2015 ; Accepted: 10 November 2015 ; Published: 16 November 2015
Academic Editor: Terrence Piva

[1] Department of Biomedical Engineering, Yonsei-Fraunhofer Medical Device Laboratory, Yonsei University, Wonju, Gangwon-do 26493, Korea; yyeongm@hanmail.net (Y.-M.Y.); hyungpump@hanmail.net (J.H.P.); seodongh@gmail.com (D.-H.S.); sangyeob.lee.90@yonsei.ac.kr (S.L.); bjung@yonsei.ac.kr (B.J.); hanskim@yonsei.ac.kr (H.S.K.)

[2] Division of Biological Science and Technology, Yonsei University, Wonju, Gangwon-do 26493, Korea; blue-me914@hanmail.net

* Correspondence: kbae@yonsei.ac.kr; Tel.: +82-33-760-2280; Fax: +82-33-760-2183

† These authors contributed equally to this work.

**Abstract:** Low-level laser therapy/treatment (LLLT) using a minimally invasive laser needle system (MILNS) might enhance bone formation and suppress bone resorption. In this study, the use of 405 nm LLLT led to decreases in bone volume and bone mineral density (BMD) of tibial trabecular bone in wild-type (WT) and *Per2* knockout (KO) mice. Bone volume and bone mineral density of tibial trabecular bone was decreased by 405 nm LLLT in *Per2* KO compared to WT mice at two and four weeks. To determine the reduction in tibial bone, mRNA expressions of alkaline phosphatase (*ALP)* and *Per2* were investigated at four weeks after 405 nm laser stimulation using MILNS. *ALP* gene expression was significantly reduced in the LLLT-stimulated right tibial bone of WT and *Per2* KO mice compared to the non-irradiated left tibia ($p < 0.001$). *Per2* mRNA expression in WT mice was significantly reduced in the LLLT-stimulated right tibial bone compared to the non-irradiated left tibia ($p < 0.001$). To identify the decrease in tibial bone mediated by the *Per2* gene, levels of runt-related transcription factor 2 (*Runx2*) and *ALP* mRNAs were determined in non-irradiated WT and *Per2* KO mice. These results demonstrated significant downregulation of *Runx2* and *ALP* mRNA levels in *Per2* KO mice ($p < 0.001$). Therefore, the reduction in tibial trabecular bone resulting from 405 nm LLLT using MILNS might be associated with *Per2* gene expression.

**Keywords:** tibia; trabecular bone; *Per2*; *ALP*; *Runx*; low-level laser therapy; minimally invasive laser needle system

## 1. Introduction

Although the biological mechanisms of low-level laser irradiation or low-level laser therapy/treatment (LLLT) have not been fully revealed, LLLT is a successfully and widely used non-pharmacological method for bone regeneration in experimental *in vivo* and *in vitro* models [1–12]. Current research suggests that LLLT stimulates the proliferation and differentiation of various cell types and promotes the repair process *in vivo* and *in vitro*: a wavelength of 600–904 nm and an output power of 1–500 mW; activation of ERK1/ERK2 and a phosphatidylinositol 3-kinase (PI3K) pathway; the increase of reactive oxygen species (ROS) and ATP/cyclic AMP; the absorption of light by a photoreceptor and the photoactivation of enzymes in the mitochondria; *etc.* [1,2]. With respect to

bone, LLLT has been shown to modulate inflammatory processes and bone repair [3–5], accelerate osteoblast proliferation and bone formation [6–10], and enhance bone healing [1,11,12].

Low-level laser irradiation (LLLT) can scatter across the skin surface, limiting penetration to the deep bone layers. Thus, LLLT has been directly applied to the bone site of interest through tissue incision. In addition, initial photon density and therapeutic efficacy of LLLT is reduced by light-tissue interaction, such as absorption and scattering [13,14]. LLLT (660 nm wavelength) using a MILNS has been developed to overcome these light limitations in tissue. The effectiveness of this technique for preventing trabecular bone loss has been demonstrated in previous research [13,15,16].

The circadian clock genes *Period 2* (*Per2*) and *Cryptochrome 2* (*Cry2*) regulate distinct pathways in bone volume; *Cry2* chiefly influences the osteoclasts, and *Per2* acts on osteoblasts, indicating that *Per2* and *Cry2* differentially balance bone formation [17,18]. Mammalian Cry protein with flavin adenine dinucleotide (FAD) serves as a blue-light photoreceptor of 405 nm wavelength in murine cells [19,20]. The Kushibiki group has shown that LLLT (405 nm) can promote osteogenesis and reduce adipogenesis of mouse mesenchymal stromal cells (MSCs) by inducing translocation of Cry1 and Per2 proteins and decreasing *Cry1* mRNA level. LLLT can effectively control the *in vitro* fate of MSCs as a therapeutic strategy by suppressing Cry transcription [19,20]. Therefore, the present study demonstrated that 405 nm laser stimulation using MILNS applied *in vivo* tibial trabecular bone in WT and *Per2* gene KO mice to investigate bone volume and BMD with an *in vivo* micro-CT and expressions of *Per2*, *Runx2*, and *ALP* mRNAs through real-time quantitative polymerase chain reaction.

## 2. Results

The structural parameters to quantify tibial trabecular bone changes using micro-CT systems were shown in the 405 nm laser-irradiated WT and *Per2* KO mice, respectively (Figure 1). The bone microarchitecture values of BV/TV, Tb.Sp, Tb.N, Conn.Dn, and BMD were significantly changed in the 405 nm laser-irradiated WT and *Per2* KO mice at four weeks compared to two weeks, respectively (BV/TV, Tb.Sp, and Tb.N, $p < 0.01$; Conn.Dn and BMD, $p < 0.001$) (Figure 1). Three-dimensional (3D) images of decreased trabecular bone were seen in *Per2* KO mice compared to WT mice that received 405 nm laser irradiation at 0, 2 and 4 weeks (Figure 2A). Changes in structural parameters were evaluated with total bone volume and BMD in WT mice and *Per2* KO mice at 0, 2 and 4 weeks (Figure 2B,C). Total bone volume and BMD were significantly reduced in *Per2* KO mice compared to WT mice ($p < 0.001$).

To measure the reduction of tibial bone affected by LLLT using MILNS, levels of *ALP* and *Per2* mRNA were investigated in the 405 nm laser-irradiated WT and *Per2* KO mice at four weeks, respectively (Figure 3). *ALP* mRNA level was significantly reduced in right tibial bone of WT and *Per2* KO mice compared to left tibia, respectively ($p < 0.001$) (Figure 3A). In addition, *Per2* mRNA level in WT mice was significantly lower in right tibial bone compared to left tibia ($p < 0.001$) (Figure 3B).

To identify the decrease in tibial trabecular bone via *Per2* gene, levels of *Runx2* and *ALP* mRNA were determined in non-irradiated WT and *Per2* KO mice, demonstrating significant down-regulation of *Runx2* and *ALP* mRNA levels in *Per2* KO mice compared to WT mice ($p < 0.001$) (Figure 4A,B). *Per2* mRNA was expressed in WT mice and was not detected in *Per2* KO mice (Figure 4C). Therefore, the reduction in tibial trabecular bone by 405 nm laser irradiation according to MILNS might be associated with *Per2* genes.

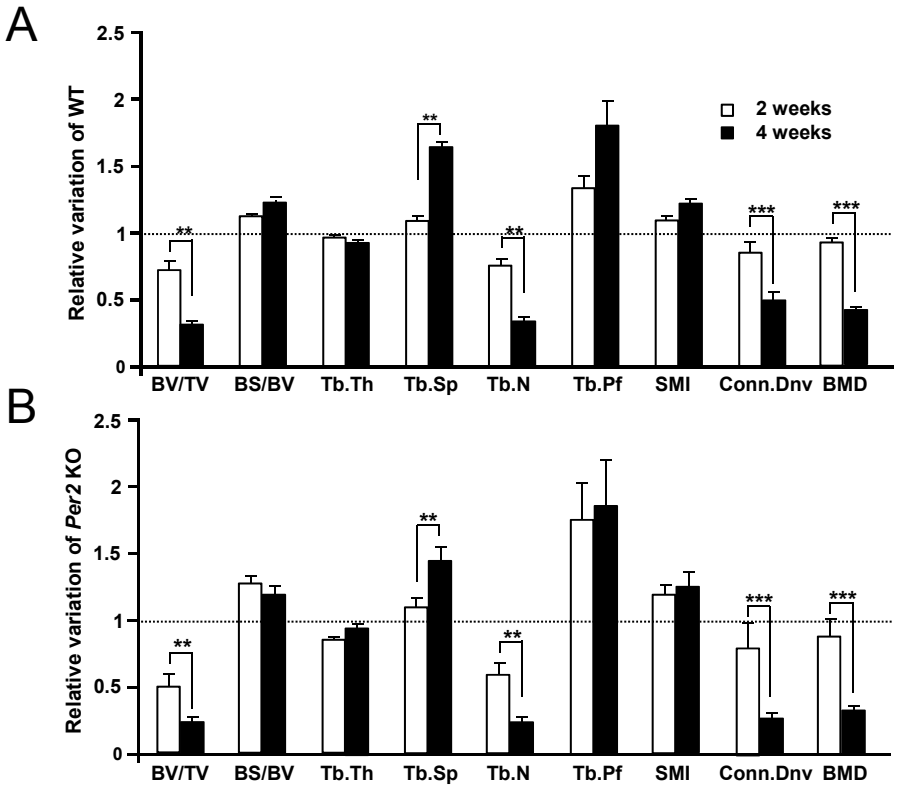


**Figure 1.** Structural parameters in 405 nm LLLT using MILNS in WT (**A**) and *Per2* KO mice (**B**), respectively. Trabecular bone parameters measured with micro-CT and depicted as a histogram. Dotted line indicates relative variation at the start of LLLT using MILNS. The tibia was directly irradiated with LLLT using the MILNS (405 nm, 5 mW, 3 J/cm$^2$, 600 s). Mice were irradiated five days/week for four weeks. At two and four weeks after laser irradiation, BV/TV (%), Tb.Th (mm), Tb.Sp (mm), Tb.N (mm$^{-1}$), Tb.Pf (mm$^{-1}$), SMI, Conn.Dn (mm$^{-3}$), and BMD (g/cm$^3$) were measured from two-dimensional images obtained using CT-AN 1.8. Data are expressed as mean ± SEM ($n$ = 9) at each point and were subjected to statistical analysis, ** $p < 0.01$; ***$p < 0.001$. LLLT: Low-level laser therapy/treatment; MILNS: minimally invasive laser needle system; WT: wild-type; BV/TV: structural parameters including bone volume fraction; Tb.Th: trabecular thickness; Tb.Sp: trabecular separation; Tb.N: trabeculae number; Tb.Pf: trabecular bone pattern factor; SMI: structure model index; Conn.Dn: connective density; BMD: bone mineral density.

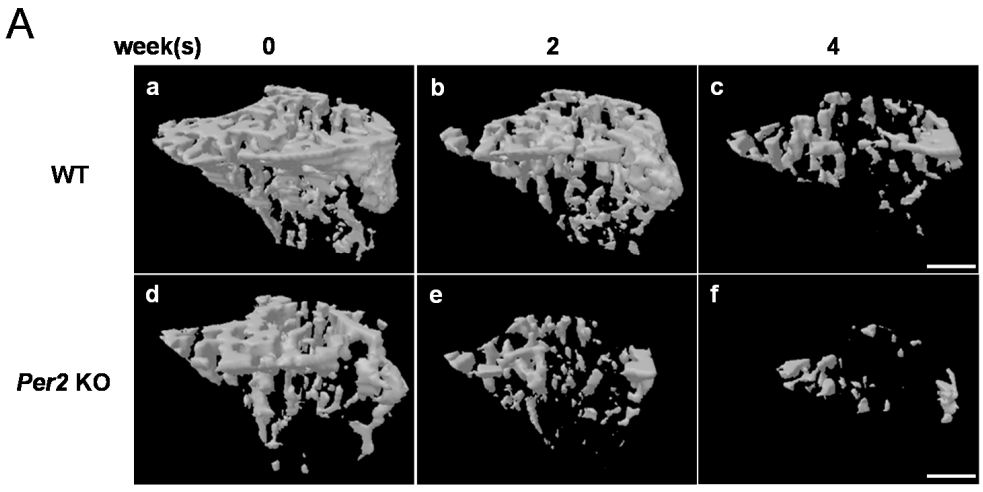


**Figure 2.** *Cont.*

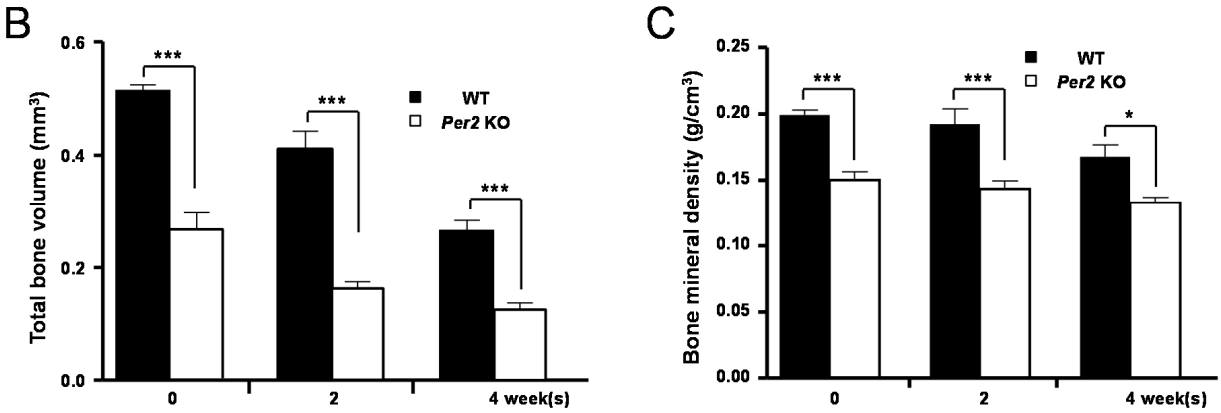


**Figure 2.** (**A**) Representative longitudinal 3D micro-CT images showing changes in right trabecular bone microarchitecture regions of interest in 405 nm LLLT using MILNS in WT and *Per2* KO mice: (**A**) **a** and **d**, 0 weeks; **b** and **e**, two weeks; and **c** and **f**, four weeks. The tibia was directly irradiated with LLLT using the MILNS (405 nm, 5 mW, 3 J/cm$^2$, 600 s). Mice were irradiated five days/week for four weeks. Scale bar, 0.5 mm; At 0, two, and four weeks after laser irradiation, total bone volume (mm$^3$) (**B**) and bone mineral density (g/cm$^3$) (**C**) were measured on two-dimensional images obtained using CT-AN 1.8. Data are expressed as mean ± SEM ($n$ = 9) and were subjected to statistical analysis, * $p < 0.05$; *** $p < 0.001$.

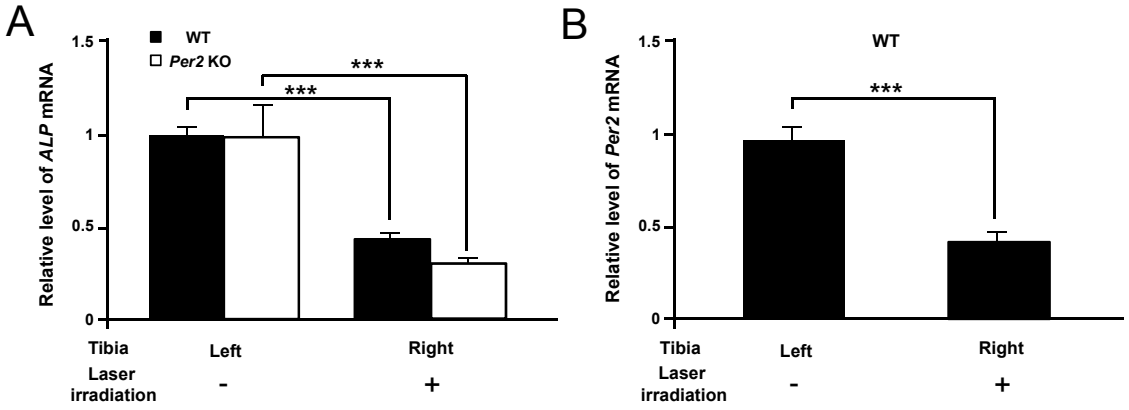


**Figure 3.** The expressions of *ALP* (**A**) and *Per2* (**B**) mRNAs in tibial bone marrows of WT and *Per2* KO mice, respectively, in 405 nm LLLT using MILNS. The data are mean ± SEM ($n$ = 3). Statistical significance is indicated by *** $p < 0.001$.

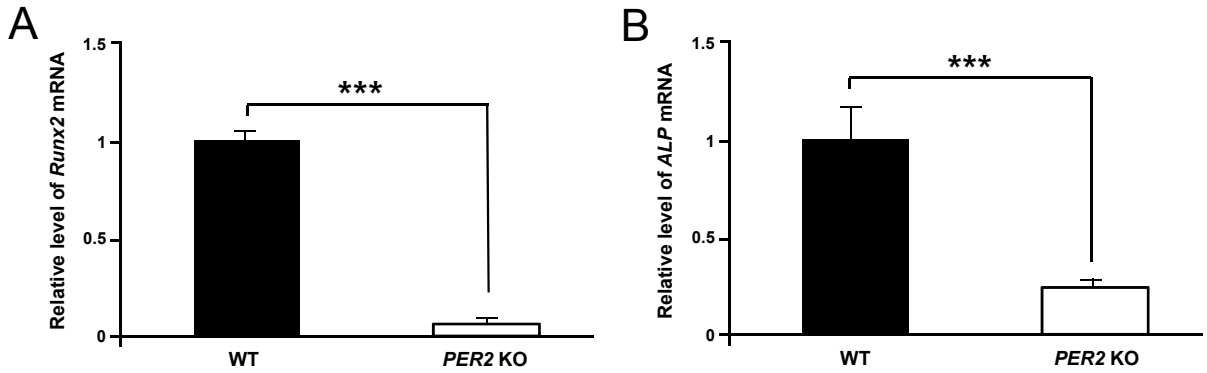


**Figure 4.** *Cont.*

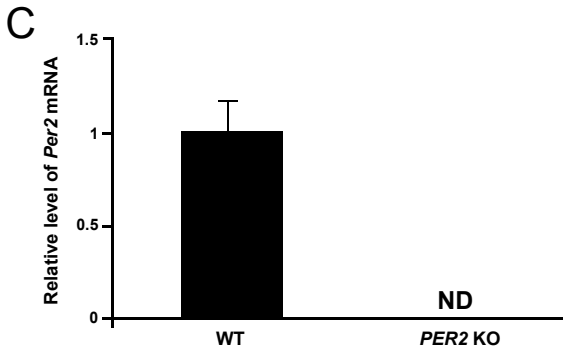


**Figure 4.** Differences in mRNA expressions of *Runx2* (**A**), *ALP* (**B**), and *Per2* (**C**) genes between tibial bone marrows of WT and *Per2* KO mice in 405 nm LLLT using MILNS. The data are mean ± SEM ($n$ = 3). Statistical significant is indicated by *** $p < 0.001$. ND, no detection.

## 3. Discussion

*In vivo*, Micro-CT system is an effective and noninvasive method for the evaluation of microstructural characteristics of bone tissues. Using micro-CT allows for clear and accurate imaging of internal and external bone structures in the smallest bone fraction [21–24]. The internal and external architecture of bone has a major impact on its mechanical properties. The mechanical properties of cancellous bone are relevant to its stiffness and strength [21–24]. The biomechanical stiffness and strength of bone depend on both bone internal architecture and BMD [25]. This study was evaluated by several structural parameters including tibial trabecular bone volume fraction (BV/TV), trabecular separation (Tb.Sp), trabecular number (Tb.N), and connective density (Conn.Dn) (Figure 1) as well as total bone volume (Figure 2B) and BMD (Figure 2C). Bone densitometry using quantitative micro-CT systems provides clinical information about BMD implicated in the BV/TV. Both BMD and BV/TV can estimate the stiffness and strength of normal and pathologic trabecular bone induced by osteoporosis or metastatic cancer [26]. BMD has also been used clinically to evaluate osteoporosis and fracture risk [27]. Our findings demonstrated that total changes in total bone volume and BMD from trabecular bone of right tibia were significantly reduced in *Per2* KO mice compared to in WT mice due to 405 nm LLLT according to MILNS at 0 to four weeks (Figure 2B,C). The 3D images obtained from micro-CT clearly identified decreased trabecular bone of right tibia in *Per2* KO mice compared to in WT mice (Figure 2A). This result suggests that the reduction in tibial trabecular bone caused by 405 nm LLLT using MILNS is mediated by the *Per2* gene. Unfortunately, this study is lack of micro-CT analysis in the trabecular bone of left tibia. However, we showed that the expressions of *ALP* mRNA was significantly different between the right and left tibial bones (Figure 3A)

This study used micro-CT data to demonstrate that LLLT using MILNS led to significant reductions in tibial trabecular bone. Our results are contrary to previous studies that reported the capability of LLLT using MILNS to stimulate the cortical bone growth of osteoporotic mice, prevent trabecular bone loss in ovariectomized mice, and suppress trabecular bone loss induced by skeletal unloading [13,15,16]. These previous studies reported that LLLT using MILNS has potential to inhibit bone loss at a wavelength of 660 nm, energy of 3 J/cm$^2$, output power of 10 mW, and irradiation time 300 s for five days per week for two weeks, indicating that it enhances bone formation and suppresses bone resorption. However, the present study applied a wavelength of 405 nm, energy of 3 J/cm$^2$, output power of 5 mW, and irradiation time of 600 s for five days per week for two and four weeks (Figure 2B,C). The other experiment also demonstrated decreased trabecular bone loss at a wavelength of 405 nm, energy of 3 J/cm$^2$, output power of 10 mW, and irradiation time 300 s (data not shown). However, the Kushibiki group used a wavelength of 405 nm, 100 mW/cm$^2$, 180 s, and two weeks and demonstrated that LLLT enhanced mesenchymal stromal cell differentiation to osteoblasts *in vitro* [19,20]. Therefore, an excessively high laser dosage might

lead to inhibitory effects on cell growth and proliferation [28–30]. Two reviews have reported that LLLT at wavelengths ranging from 600 to 904 nm and output powers of 1–500 mW is very helpful in enhancing the proliferation of various cell lines and improving bone healing [1,2]. Tajali *et al.* [3] performed a meta-analysis through MEDLINE, EMBASE, PubMed, CINAHL, and Cochrane Database of Randomized Clinical Trials published from 1966 to October 2008. Specifically, they looked for studies that highlighted the effects of LLLT on biomechanical properties of bone regeneration and the dose impact in animals. These reports might provide sufficient evidence to support the role of LLLT in animal and human bone healing.

The role of the *Per2* gene in bone is not clear, but previous studies have shown that *Per2* plays a significant role in regulating bone growth [17,18]. *Per2* KO mice demonstrate increases in bone mass and bone volume [17,18]. In children with Smith-Magenis syndrome, a genetic disorder associated with skeletal malformations, the *Per2* gene is also expressed with high variability and no *Per2* rhythm [31]. *Per2* might also influence bone growth by altering p21 cell cycle progression, through its effects on ER-mediated gene expression and its action on parathyroid hormone administration [32–34]. However, in the present study, *Per2* KO mice showed significantly reduced bone volume and BMD in tibial trabecular bone due to LLLT using MILNS (Figures 1 and 2B,C).

Runt-related transcription factor 2 (*Runx2*) is a master transcription factor of osteoblast differentiation or osteogenesis. *Runx2* expression is upregulated in immature osteoblasts, decreases during bone development, and demonstrates a mature phenotype in osteoblasts, which are required for mature bone formation [35,36]. *ALP* plays an essential role in the bone formation process and reflects osteoblastic activity [37,38]. *ALP* is used clinically as a marker of bone formation. LLLT has a biostimulatory effect on bone formation and increases *ALP* expression or activity. Previous studies have shown that LLLT induces a significant increase in expression of *Runx2* and *ALP* mRNAs [4,39–43]. LLLT effects on osteoblast proliferation and bone formation involving the increase of *Runx2* mRNA [6,8]. The present study, however, demonstrated that *Per2* KO mice rather than WT mice significantly downregulated *Runx2* and *ALP* mRNA levels in tibial trabecular bone after LLLT using MILNS (Figure 4). This finding indicates that the reduction of *Runx2* and *ALP* mRNA levels in the tibial trabecular bone caused by 405 nm laser irradiation using MILNS is associated with the decrease of *Per2* gene expression.

## 4. Experimental Section

### *4.1. Experimental Animals*

All procedures were performed according to a protocol approved by the Yonsei University of Animal Care Committee (YMC-141112-1). Male inbred 129/Sv WT and *mPer2* KO mice at 6 weeks of age (average weight 24.2 $\pm$ 0.8 g) ($n$ = 9) were maintained in the animal facility of Yonsei University, Wonju, Korea. Environment of cage was controlled within standard conditions, temperature (23.5 $\pm$ 1 °C) and humidity (50% $\pm$ 5%). And also the mice were in controlled light (12:12 h light/dark (LD) schedule; light on at 7:00 a.m.), and were fed *ad libitum*. Mice were stabilized and synchronized with LD cycle in time-scheduled animal facility for at least 2 weeks.

### *4.2. LLLT Using MILNS*

In this study, laser stimulation was performed using the MILNS technique previously developed by the Department of Biomedical Engineering and Yonsei-Fraunhofer Medical Device Lab [13,15,16]. A 130-μm-inner diameter fine needle was used to guide a 100-μm-diameter optical fiber. A diode laser (120 mW, 405 nm; No. ML320G2-11; ThorLabs, Newton, NJ, USA) was used as a light source. The optical power output from the diode laser at the end of the fine needle was set to 10 mW just before irradiation of the bone. The tibia was directly irradiated with the laser (405 nm, 5 mW) for 600 s (energy 3 J/cm$^2$). The bone surface of the right tibia was directly irradiated percutaneously using MILNS at the proximal end of the tibia. The left tibia was not irradiated, but treated with

needle. Mice immobilized by a customized restrainer were treated 5 days per week for 2 or 4 weeks without anesthesia.

### *4.3. Measurements of Structural Parameters*

We scanned the tibiae before laser stimulation and after 2 or 4 weeks of laser stimulation with an *in vivo* micro-CT (Skyscan 1076; Bruker, Belgium, Germany) at a resolution of 18 $\mu m^3$ under anesthesia. Anesthesia, using a combination of xylazine (0.5 mL/kg; Bayer Korea, Seoul, Korea) and zoletil (0.5 mL/kg; Virbac, Seoul, Korea), was performed during micro-CT scanning. To estimate the effects of LLLT, structural parameters of tibia were quantitatively measured. The structural parameters such as bone volume fraction (BV/TV, %), trabecular thickness (Tb.Th, mm), trabecular separation (Tb.Sp, mm), trabecular number per unit length (Tb.N, $mm^{-1}$), trabecular bone pattern factor (Tb.Pf, $mm^{-1}$), structure model index (SMI), connective density (Conn.Dn, $mm^{-3}$), and bone mineral density (BMD, $g/cm^3$) were analyzed on two-dimensional images obtained by CT-AN 1.8 (Bruker, Germany). We selected the region of interest (ROI) for microCT analyses, 1.8 mm in length at the distal metaphyseal secondary spongiosa (100 slices) from a point that is under 0.54 mm (30 slices) from the end of the proximal growth plate on the tibia.

### *4.4. Preparation of cDNA and Real-Time Quantitative Polymerase Chain Reaction (qPCR)*

Total RNAs from tibial bone marrow were isolated from mice sacrificed at 4 weeks after LLLT. Total RNA from each sample was extracted using TRI reagent (MRC, Cincinnati, OH, USA), following the manufacturer's instructions. Samples in 100 μL of TRI reagent were homogenized, and any contaminating genomic DNA was eliminated using the RNase-Free DNase kit (Promega, Madison, WI, USA). GoScript™ Reverse Transcription System (Promega) was used to synthesize cDNA from 2 μg of total RNA, according to the manufacturer's protocol. The *gapdh* housekeeping gene was used as a constitutive control for normalization. The specific primer pairs used for real-time PCR are listed in Table 1. qPCR were carried out using SYBR Green reagent (Applied Biosystems, Foster City, CA, USA) and the StepOnePlus Systems (Applied Biosystems). PCR conditions included one cycle of 10 min at 95 °C followed by 40 cycles of 15 s at 95 °C, 30 s at 58 °C, and 30 s at 72 °C. The relative gene expression level was calculated using the $2^{-\triangle\triangle Ct}$ method [44]. All samples were analyzed in triplicate and in three independent measures.

**Table 1.** Nucleotide sequences of the primer pairs used for real-time PCR.

| Gene | Strand | Sequence | Accession No. |
|---|---|---|---|
| *Runx2* | Forward | 5′-TAG CCA GGT TCA ACG ATC TG-3′ | NM001145920.2 |
| | Reverse | 5′-TTC TGT CTG TGC CTT CTT GG-3′ | |
| *ALP* | Forward | 5′-ATA TAA CAC CAA CGC TCA GG-3′ | NM007431.3 |
| | Reverse | 5′-AGG ATG GAT GTG ACC TCA TT-3′ | |
| *Per2* | Forward | 5′-TAT CGT GAA GAA CGC GGA TA-3′ | NM011066.3 |
| | Reverse | 5′-AGC TGT GGA ACA CAC TGA CG-3′ | |
| *Gapdh* | Forward | 5′-GAC ATC AAG AAG GTG GTG AAG C-3′ | NM008084.3 |
| | Reverse | 5′-GAA GGT GGA AGA GTG GGA GTT-3′ | |

### *4.5. Statistical Analysis*

All the experiments were carried out at least three times. Data are presented as mean ± standard error of the mean (SEM). The significance of differences between groups was determined using Student's *t*-test with SPSS 17.0 (SPSS Inc., Chicago, IL, USA). *p*-values less than 0.05 were considered statistically significant.

## 5. Conclusions

The results of our study illustrate that LLLT using MILNS plays a critical role in the decrease of bone volume and BMD in tibial trabecular bone in WT and *Per2* KO mice. This reduction of bone depended on significant downregulation of *Runx2* and *ALP* mRNA levels in *Per2* KO mice compared to WT mice. Future research should investigate whether specific pharmaceutical targeting of the *Per2* gene can serve as a new therapeutic avenue to treat bone loss conditions such as osteoporosis.

**Acknowledgments:** This research was supported by the Leading Foreign Research Institute Recruitment Program through the National Research Foundation of Korea (NRF) funded by the Ministry of Science, ICT & Future Planning (2010-00757).

**Author Contributions:** Yeong-Min Yoo and Kiho Bae contributed to the analysis of the study and manuscript writing; Myung-Han Lee contributed to the conception and instruction of the study; Ji Hyung Park and Dong-Hyun Seo performed the data analysis; and Sangyeob Lee, Byungjo Jung and Han Sung Kim provided critical comment on the content of the review.

**Conflicts of Interest:** The authors declare no conflict of interest.

## References

1. Ebrahimi, T.; Moslemi, N.; Rokn, A.; Heidari, M.; Nokhbatolfoghahaie, H.; Fekrazad, R. The influence of low-intensity laser therapy on bone healing. *J. Dent.* **2012**, *9*, 238–248.
2. Al Ghamdi, K.M.; Kumar, A.; Moussa, N.A. Low-level laser therapy: A useful technique for enhancing the proliferation of various cultured cells. *Lasers Med. Sci.* **2012**, *27*, 237–249. [CrossRef] [PubMed]
3. Tajali, B.S.; Macdermid, J.C.; Houghton, P.; Grewal, R. Effects of low power laser irradiation on bone healing in animals: A meta-analysis. *J. Orthop. Surg. Res.* **2010**, *5*, 1–10. [CrossRef] [PubMed]
4. Fernandes, K.R.; Ribeiro, D.A.; Rodrigues, N.C.; Tim, C.; Santos, A.A.; Parizotto, N.A.; de Araujo, H.S.; Driusso, P.; Rennó, A.C. Effects of low-level laser therapy on the expression of osteogenic genes related in the initial stages of bone defects in rats. *J. Biomed. Opt.* **2013**, *18*, 038002. [CrossRef] [PubMed]
5. Sella, V.R.; do Bomfim, F.R.; Machado, P.C.; da Silva Morsoleto, M.J.; Chohfi, M.; Plapler, H. Effect of low-level laser therapy on bone repair: A randomized controlled experimental study. *Lasers Med. Sci.* **2015**, *30*, 1061–1068. [CrossRef] [PubMed]
6. Grassi, F.R.; Ciccolella, F.; d'Apolito, G.; Papa, F.; Iuso, A.; Salzo, A.E.; Trentadue, R.; Nardi, G.M.; Scivetti, M.; de Matteo, M.; *et al*. Effect of low-level laser irradiation on osteoblast proliferation and bone formation. *J. Biol. Regul. Homeost. Agents* **2011**, *25*, 603–614. [PubMed]
7. Jawad, M.M.; Husein, A.; Azlina, A.; Alam, M.K.; Hassan, R.; Shaari, R. Effect of 940 nm low-level laser therapy on osteogenesis *in vitro*. *J. Biomed. Opt.* **2013**, *18*. [CrossRef] [PubMed]
8. Kiyosaki, T.; Mitsui, N.; Suzuki, N.; Shimizu, N. Low-level laser therapy stimulates mineralization via increased *Runx2* expression and ERK phosphorylation in osteoblasts. *Photomed. Laser Surg.* **2010**, *28* (Suppl. 1), S167–S172. [CrossRef] [PubMed]
9. Ghahroudi, A.A.R.; Rokn, A.R.; Kalhori, K.A.; Khorsand, A.; Pournabi, A.; Pinheiro, A.L.; Fekrazad, R. Effect of low-level laser therapy irradiation and Bio-Oss graft material on the osteogenesis process in rabbit calvarium defects: A double blind experimental study. *Lasers Med. Sci.* **2014**, *29*, 925–932. [CrossRef] [PubMed]
10. Scalize, P.H.; de Sousa, L.G.; Regalo, S.C.; Semprini, M.; Pitol, D.L.; da Silva, G.A.; de Almeida Coelho, J.; Coppi, A.A.; Laad, A.A.; Prado, K.F.; *et al*. Low-level laser therapy improves bone formation: Stereology findings for osteoporosis in rat model. *Lasers Med. Sci.* **2015**, *30*, 1599–1607. [CrossRef] [PubMed]
11. Batista, J.D.; Sargenti-Neto, S.; Dechichi, P.; Rocha, F.S.; Pagnoncelli, R.M. Low-level laser therapy on bone repair: Is there any effect outside the irradiated field? *Lasers Med. Sci.* **2015**, *30*, 1569–1574. [CrossRef] [PubMed]
12. Aras, M.H.; Erkilic, S.; Demir, T.; Demirkol, M.; Kaplan, D.S.; Yolcu, U. Effects of low-level laser therapy on osteoblastic bone formation and relapse in an experimental rapid maxillary expansion model. *Niger J. Clin. Pract.* **2015**, *18*, 607–611. [PubMed]

13. Kang, H.; Ko, C.Y.; Ryu, Y.; Seo, D.H.; Kim, H.S.; Jung, B. Development of a minimally invasive laser needle system: Effects on cortical bone of osteoporotic mice. *Lasers Med. Sci.* **2012**, *27*, 965–969. [CrossRef] [PubMed]
14. Ninomiya, T.; Hosoya, A.; Nakamura, H.; Sano, K.; Nishisaka, T.; Ozawa, H. Increase of bone volume by a nanosecond pulsed laser irradiation is caused by a decreased osteoclast number and an activated osteoblasts. *Bone* **2007**, *40*, 140–148. [CrossRef] [PubMed]
15. Ko, C.Y.; Kang, H.; Seo, D.H.; Jung, B.; Schreiber, J.; Kim, H.S. Low-level laser therapy using the minimally invasive laser needle system on osteoporotic bone in ovariectomized mice. *Med. Eng. Phys.* **2013**, *35*, 1015–1019. [CrossRef] [PubMed]
16. Ko, C.Y.; Kang, H.; Ryu, Y.; Jung, B.; Kim, H.; Jeong, D.; Shin, H.I.; Lim, D.; Kim, H.S. The effects of minimally invasive laser needle system on suppression of trabecular bone loss induced by skeletal unloading. *Lasers Med. Sci.* **2013**, *28*, 1495–1502. [CrossRef] [PubMed]
17. Fu, L.; Patel, M.S.; Bradley, A.; Wagner, E.F.; Karsenty, G. The molecular clock mediates leptin-regulated bone formation. *Cell* **2005**, *122*, 803–815. [CrossRef] [PubMed]
18. Maronde, E.; Schilling, A.F.; Seitz, S.; Schinke, T.; Schmutz, I.; van der Horst, G.; Amling, M.; Albrecht, U. The clock genes *Period 2* and *Cryptochrome 2* differentially balance bone formation. *PLoS ONE* **2010**, *5*, e11527. [CrossRef] [PubMed]
19. Kushibiki, T.; Awazu, K. Controlling osteogenesis and adipogenesis of mesenchymal stromal cells by regulating a circadian clock protein with laser irradiation. *Int. J. Med. Sci.* **2008**, *5*, 319–326. [CrossRef] [PubMed]
20. Kushibiki, T.; Hirasawa, T.; Okawa, S.; Ishihara, M. Low reactive level laser therapy for mesenchymal stromal cells therapies. *Stem Cells Int.* **2015**, *2015*, 974864. [CrossRef] [PubMed]
21. Dougherty, G. Quantitative CT in the measurement of bone quantity and bone quality for assessing osteoporosis. *Med. Eng. Phys.* **1996**, *18*, 557–568. [CrossRef]
22. Hohlweg-Majert, B.; Pautke, C.; Deppe, H.; Metzger, M.C.; Wagner, K.; Schulze, D. Qualitative and quantitative evaluation of bony structures based on DICOM dataset. *J. Oral Maxillofac. Surg.* **2011**, *69*, 2763–2770. [CrossRef] [PubMed]
23. Munakata, M.; Tachikawa, N.; Honda, E.; Shiota, M.; Kasugai, S. Influence of menopause on mandibular bone quantity and quality in Japanese women receiving dental implants. *Arch. Osteoporos.* **2011**, *6*, 51–57. [CrossRef] [PubMed]
24. Tolstunov, L.; Thai, D.; Arellano, L. Implant-guided volumetric analysis of edentulous maxillary bone with cone beam CT scan. Maxillary sinus pneumatization classification. *J. Oral Implantol.* **2012**, *38*, 377–390. [CrossRef] [PubMed]
25. Langton, C.M.; Pisharody, S.; Keyak, J.H. Comparison of 3D finite element analysis derived stiffness and BMD to determine the failure load of the excised proximal femur. *Med. Eng. Phys.* **2009**, *31*, 668–672. [CrossRef] [PubMed]
26. Nazarian, A.; von Stechow, D.; Zurakowski, D.; Müller, R.; Snyder, B.D. Bone volume fraction explains the variation in strength and stiffness of cancellous bone affected by metastatic cancer and osteoporosis. *Calcif. Tissue Int.* **2008**, *83*, 368–379. [CrossRef] [PubMed]
27. Zbranca, E.; Galusca, B.; Mogos, V. Bone mineral densitometry. The importance of BMD in endocrinologist practice. *Timisoara Med. J.* **2004**, *3*, 260–267.
28. Gross, A.J.; Jelkmann, W. Helium-neon laser irradiation inhibits the growth of kidney epithelial cells in culture. *Lasers Surg. Med.* **1990**, *10*, 40–44. [CrossRef] [PubMed]
29. Sattayut, S.; Hughes, F.; Bradly, P. 820 nm gallium aluminium arsenide laser modulation of prostaglandin E2 production in interleukin-1 stimulated myoblasts. *Laser Ther.* **1999**, *11*, 88–95. [CrossRef]
30. Shu, B.; Ni, G.X.; Zhang, L.Y.; Li, X.P.; Jiang, W.L.; Zhang, L.Q. High-power helium-neon laser irradiation inhibits the growth of traumatic scars *in vitro* and *in vivo*. *Lasers Med. Sci.* **2013**, *28*, 693–700. [CrossRef] [PubMed]
31. Nováková, M.; Nevsímalová, S.; Príhodová, I.; Sládek, M.; Sumová, A. Alteration of the circadian clock in children with Smith-Magenis syndrome. *J. Clin. Endocrinol. Metab.* **2012**, *97*, E312–E318. [CrossRef] [PubMed]

32. Gu, X.; Xing, L.; Shi, G.; Liu, Z.; Wang, X.; Qu, Z.; Wu, X.; Dong, Z.; Gao, X.; Liu, G.; *et al*. The circadian mutation PER2 (S662G) is linked to cell cycle progression and tumorigenesis. *Cell Death Differ.* **2012**, *19*, 397–405. [CrossRef] [PubMed]
33. Gery, S.; Virk, R.K.; Chumakov, K.; Yu, A.; Koeffler, H.P. The clock gene *Per2* links the circadian system to the estrogen receptor. *Oncogene* **2007**, *26*, 7916–7920. [CrossRef] [PubMed]
34. Okubo, N.; Fujiwara, H.; Minami, Y.; Kunimoto, T.; Hosokawa, T.; Umemura, Y.; Inokawa, H.; Asada, M.; Oda, R.; Kubo, T.; *et al*. Parathyroid hormone resets the cartilage circadian clock of the organ-cultured murine femur. *Acta Orthop.* **2015**, 1–5. [CrossRef] [PubMed]
35. Komori, T. Regulation of osteoblast differentiation by *Runx2*. *Adv. Exp. Med. Biol.* **2010**, *658*, 43–49. [PubMed]
36. Vimalraj, S.; Arumugam, B.; Miranda, P.J.; Selvamurugan, N. *Runx2*: Structure, function, and phosphorylation in osteoblast differentiation. *Int. J. Biol. Macromol.* **2015**, *78*, 202–208. [CrossRef] [PubMed]
37. Golub, E.E.; Boesze-Battaglia, K. The role of alkaline phosphatase in mineralization. *Curr. Opin. Orthop.* **2007**, *18*, 444–448. [CrossRef]
38. Christenson, R.H. Biochemical markers of bone metabolism: An overview. *Clin. Biochem.* **1997**, *30*, 573–593. [CrossRef]
39. Stein, E.; Koehn, J.; Sutter, W.; Wendtlandt, G.; Wanschitz, F.; Thurnher, D.; Baghestanian, M.; Turhani, D. Initial effects of low-level laser therapy on growth and differentiation of human osteoblast-like cells. *Wien. Klin. Wochenschr.* **2008**, *120*, 112–117. [CrossRef] [PubMed]
40. Ozawa, Y.; Shimizu, N.; Kariya, G.; Abiko, Y. Lowenergy laser irradiation stimulates bone nodule formation at early stages of cell culture in rat calvarial cells. *Bone* **1998**, *22*, 347–354. [CrossRef]
41. Ueda, Y.; Shimizu, N. Effects of pulse frequency of low-level laser therapy (LLLT) on bone nodule formation in rat calvarial cells. *J. Clin. Laser Med. Surg.* **2003**, *21*, 271–277. [CrossRef] [PubMed]
42. Wu, J.Y.; Chen, C.H.; Yeh, L.Y.; Yeh, M.L.; Ting, C.C.; Wang, Y.H. Low-power laser irradiation promotes the proliferation and osteogenic differentiation of human periodontal ligament cells via cyclic adenosine monophosphate. *Int. J. Oral Sci.* **2013**, *5*, 85–91. [CrossRef] [PubMed]
43. Hirata, S.; Kitamura, C.; Fukushima, H.; Nakamichi, I.; Abiko, Y.; Terashita, M.; Jimi, E. Low-level laser irradiation enhances BMP-induced osteoblast differentiation by stimulating the BMP/Smad signaling pathway. *J. Cell. Biochem.* **2010**, *111*, 1445–1452. [CrossRef] [PubMed]
44. Livak, K.J.; Schmittgen, T.D. Analysis of relative gene expression data using real-time quantitative PCR and the 2(-Delta Delta C(T)) Method. *Methods* **2001**, *25*, 402–408. [CrossRef] [PubMed]